Volumetric Local SAR Mapping for Parallel Transmission

L. Alon[1], C. M. Deniz[1], J. Xu[2,3], R. Brown[1], D. K. Sodickson[1], and Y. Zhu[1]

[1]Center for Biomedical Imaging, Department of Radiology, NYU School of Medicine, New York, NY, United States, [2]Center for Biomedical Imaging, Department of Radiology, NYU School of Medicine, New York, United States, [3]Siemens Medical Solutions, Malvern, PA, United States

Introduction: In this study, a custom pulse sequence was implemented to streamline volumetric local SAR mapping in parallel transmit systems. This sequence combines MR thermometry and RF heating to determine the local electric field covariance matrix Λ_r, thus allowing the prediction of true local SAR for any transmit pulse weighting. The developed pulse sequence integrated the following processes required for local SAR mapping: 1) pre-heating GRE phase map acquisition, 2) RF heating period, 3) post-heating GRE phase map acquisition, 4) delay time to allow cooling. The sequence reduces manual intervention required to assess local SAR, which can be especially tedious for many-element transmit arrays since the number of required measurements is equal to the square of the number of coils.

Theory and Methods: In this work, local SAR induced by a three-channel transmit coil was mapped in an agar gel phantom (Figure 1) using an automated pulse sequence and post-processing. All measurements were performed on a 7T scanner (Siemens Medical Solutions, Erlangen, Germany) equipped with an 8-channel parallel transmit system. The local RF power deposition following a parallel excitation with multiple transmit coils is given by (1,2)

$$\mathrm{SAR}(r) = [w_1 \quad \dots \quad w_N]^H \left(\frac{\sigma(r)}{2\rho(r)} \begin{bmatrix} e_1(r) \\ \vdots \\ e_N(r) \end{bmatrix}^* [e_1(r) \quad \dots \quad e_N(r)] \right) \begin{bmatrix} w_1 \\ \vdots \\ w_N \end{bmatrix} = w^H \Lambda_r \, w, \qquad [1]$$

where Λ_r is the electric field covariance matrix, σ is the conductivity of the sample, ρ is the density of the sample, e_i is the unit electric field generated by the i-th coil, w_i is the complex transmit current weight, r is position, and H represents the complex-conjugate transpose. To map local SAR for the three-element transmit array, Λ_r must be determined using 3^2 calibration steps, wherein a high duty cycle RF heating pulse is applied with various weightings as shown in table 2. Three additional steps with random transmit weightings were included to test the predictive capability of the model. The weightings were defined in an external file and incorporated into the sequence before runtime. To produce measurable RF heating for this gel phantom, a high amplitude 4 ms rectangular RF pulse was applied at 25% duty cycle for 480 seconds. Gradient pulses were not applied during this period to eliminate possible gradient-induced phase drift. Before and after each RF heating cycle, temperature difference maps were acquired using the proton resonance frequency shift (PRF) method (4). Assuming that heating occurs over a for a short period, heat diffusion is insignificant (4) and thus ΔT(r) = constant*SAR(r) . The temperature maps were calculated using (4) $\Delta T(r) = \frac{\Delta\phi(r)}{\alpha \cdot TE \cdot \omega}$, where $\Delta\phi$ is the difference in unwrapped phase between 2D spoiled GRE images acquired before and after the RF heating period, α=0.01ppm/°C is the PRF change coefficient, TE = 7 ms, and ω is the larmor frequency. One transverse slice was acquired with the following parameters: TR = 60 ms, slice thickness = 8 mm, and matrix size = 128× 128. Between any two experiments no imaging or RF was played out for 9.6 minutes, to allow the phantom and coils electronics to cool off.

In summary, the developed pulse sequence integrated GRE phase mapping and RF heating to map local SAR. For the three-element transmit coil array investigated here, phase difference mapping and RF heating were repeated 9 times with predefined transmit weightings to measure Λ_r, plus three additional cycles with random transmit weightings to compare the expected temperature change to that measured using PRF.

Figure 1. The cylindrical agar gel phantom having conductivity of 0.77 S/m and permittivity of 58. The three transmit/receive coils were located under the phantom (see red arrows).

	Channel 1		Channel 2		Channel 3	
Experiment	Amplitude	Phase	Amplitude	Phase	Amplitude	Phase
1	1	0	0	0	0	0
2	0	0	1	0	0	0
3	0	0	0	0	1	0
4	1	0	1	0	0	0
5	1	0	1	90	0	0
6	0	0	1	0	1	0
7	0	0	1	0	1	90
8	1	0	0	0	1	0
9	1	0	0	0	1	90
Random 1	0.675299	45.97	0.713518	49.33	0.638502	5.763
Random 2	0.710883	15.84	0.261207	59.65	0.979791	83.83
Random 3	0.343853	34.35	0.33071	42.97	0.995513	78.1

Table 2. Weightings applied to the coils in each of the heating experiments. The first 9 steps were used to calibrate the local SAR maps for the 3 coils. In the last three steps, random weightings were applied to the heating in order to test the prediction of the model.

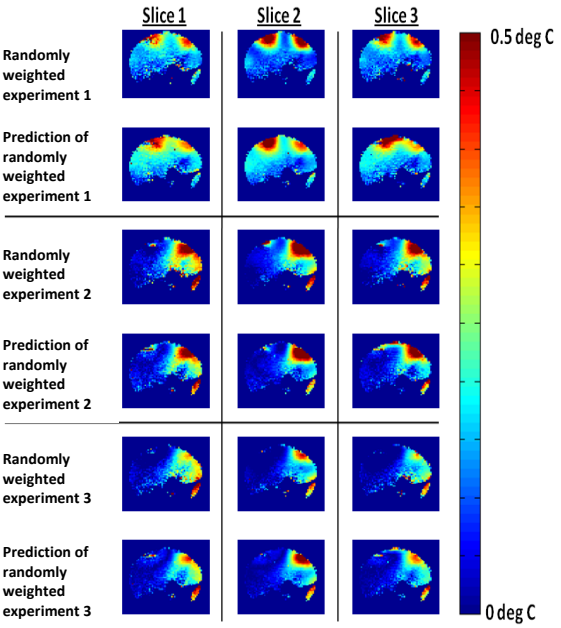

Figure 3. Random weightings were applied to the coils in the last 3 experiments, in order to confirm the model's validity. Above are the predicted and measured temperature maps for each of those three validation experiments.

Results: Temperature difference maps for each calibration step for one slice location are shown in Figure 2. The three randomly weighted experimental results are presented in figure 3. For each of the random experiments, 3 slices of measured and predicted temperature-difference maps are presented.

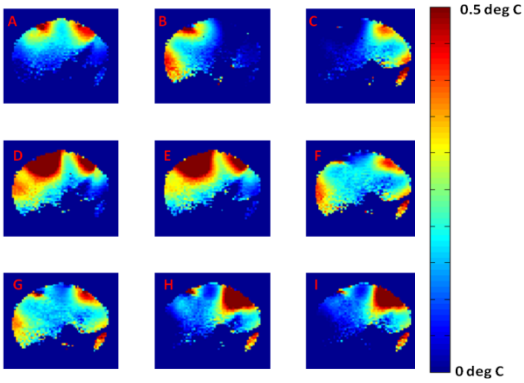

Figure 2. (A-I). Temperature difference maps in one slice. Each image corresponds to one of the first 9 experiments used to calibrate the model.

Conclusion: A streamlined pulse sequence for parallel transmit local SAR mapping in a non-perfused phantom was presented. Based on this automated calibration process, we are able to predict temperature maps that are proportional to local SAR. After the Λ_r matrices are defined for a specific configuration, local SAR maps for any pulse shape can be obtained. Future work will include increasing calibration speed, and utilization of the sequence for parallel transmit coil efficiency evaluation.

References: 1. Zhu Y. et al. In Vivo RF Power and SAR Calibration for Multi-Port RF Transmission. ISMRM 09. 2. Alon L. et al. A Local SAR Mapping Sequence for Parallel Transmission, ISMRM RF Heating Workshop 2010. 3. Zhu Y. Parallel Excitation with an Array of Transmit Coils. Magn Reson Med 2004; 51:775-784. 5.Cline H. et al. RadioFrequency Power Deposition Utilizing Thermal Imaging. Magn Reson Med 2004; 51:1129- 1137.